Resonantly Produced 7 keV Sterile Neutrino Dark Matter Models and the Properties of Milky Way Satellites

Kevork N. Abazajian

Center for Cosmology, Department of Physics and Astronomy, University of California, Irvine, Irvine, California 92697, USA

Sterile neutrinos produced through a resonant Shi-Fuller mechanism are arguably the simplest model for a dark matter interpretation of the origin of the recent unidentified x-ray line seen toward a number of objects harboring dark matter. Here, I calculate the exact parameters required in this mechanism to produce the signal. The suppression of small-scale structure predicted by these models is consistent with Local Group and high-z galaxy count constraints. Very significantly, the parameters necessary in these models to produce the full dark matter density fulfill previously determined requirements to successfully match the Milky Way Galaxy's total satellite abundance, the satellites' radial distribution, and their mass density profile, or the "too-big-to-fail problem." I also discuss how further precision determinations of the detailed properties of the candidate sterile neutrino dark matter can probe the nature of the quark-hadron transition, which takes place during the dark matter production.

Introduction.—There has been interest in dark matter having "warm" properties for a significant amount of time [1]. Interest in warm dark matter (WDM) increased in proposed solutions to the "missing satellites" problem of the Local Group of galaxies [2]. A single-particle sterile neutrino addition to the standard model of particle physics provides a minimalist extension that can be produced as a WDM particle in negligible (standard) lepton-number cosmologies through nonresonant collision-dominated production via neutrino oscillations in the early Universe in the Dodelson-Widrow mechanism [3]. This mechanism has a narrow range of parameters that fulfill the requirement of providing the observed dark matter density. Resonant Mikheyev-Smirnov-Wolfenstein (MSW)-mechanism production of sterile neutrino dark matter was found to occur in cosmologies with a small but significant lepton number through the Shi-Fuller mechanism, and the sterile neutrinos could be produced with the proper abundance with a wider range of parameters [4]. Both of these production mechanisms were forecast to have a radiative decay mode that could be detectable by x-ray telescopes as an unidentified line in observations of x-ray clusters and in field galaxies [5,6].

The Dodelson-Widrow model has recently been shown to be in significant conflict with constraints from the Local Group—namely, the galaxies' phase-space densities, their subhalo abundance, and x-ray observations of the Andromeda galaxy (M31) by Horiuchi *et al.* [7]—and it is also constrained significantly by measures of clustering in the Lyman-α (Ly-α) forest [8,9]. However, lepton-number-driven production occurs for smaller neutrino mixing angles in universes with lepton numbers significantly larger than the cosmological baryon number, which may be generated by the Affleck-Dine mechanism [10] or via massive particle decay [11]. Recently, there have been

reports of the detection of an unidentified line in stacked observations of x-ray clusters with the XMM-Newton X-ray Space Telescope with both CCD instruments aboard the telescope, and the Perseus cluster with the Chandra X-ray Space Telescope [12]. An independent group has indications of a consistent line in XMM-Newton observations of M31 and the Perseus Cluster [13]. Interestingly, these detections lie at the edge of the x-ray constraints from Horiuchi *et al.* (see Fig. 1).

In this Letter, I calculate the details of the production and perturbation evolution of resonantly produced sterile neutrino models that satisfy the signal for the best-determined parameters producing the flux of the line. The mass and rate is that determined by the 6 Ms of 73 stacked-cluster observations by the XMM-Newton MOS detector sample of Bulbul *et al.* [12]. First, I calculate the combination of lepton numbers, particle mass, and mixings required to produce the signal, which are found to be consistent with other constraints. In addition, I calculate the evolution of the perturbations of sterile neutrino dark matter through the early Universe that lead to cosmological structure formation, from large-scale structure to sub-Milky Way structure. I show that some of the parameter space in the resulting models are consistent with the Local Group constraints in Horiuchi *et al.* [7]. Furthermore, the transfer functions in the region produce a suppression in power at small scales that was found previously to be preferred to satisfy the properties of Milky Way satellites [15], including the total satellite abundance, their radial distribution, and their mass profile [16–18]. The last has been dubbed the "too-big-to-fail problem" since the halos in the models with the full cold dark matter (CDM) power produce halos with densities that should not fail to produce Milky Way satellite galaxies, but are, in turn, not seen.
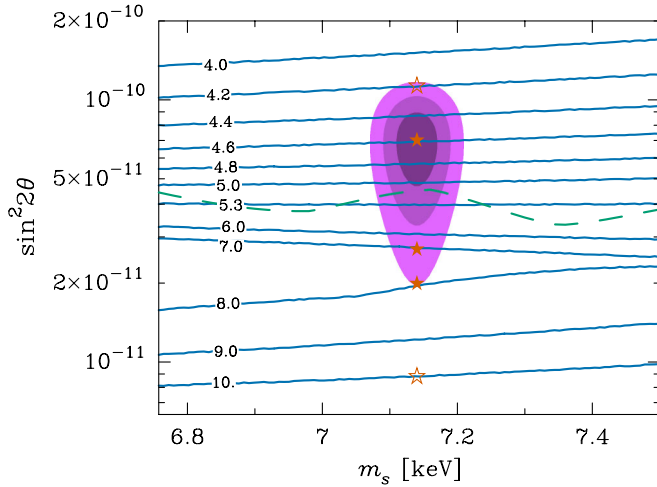
FIG. 1 (color online). This illustrates the parameter space for Shi-Fuller resonant-production sterile neutrino models in the region of interest for producing the unidentified 3.57 keV x-ray line. The filled colored contours are the 1, 2, and 3σ regions satisfying the best-determined unidentified line flux in the 6 Ms XMM-Newton 73 stacked-cluster sample of Bulbul et al. [12]. Systematic uncertainties on the flux and mixing angle are of order the 2σ uncertainties. The blue, approximately horizontal contours are labeled by the lepton number L_4, in units of 10^{-4}, needed to produce $\Omega_{\rm DM}h^2 = 0.119$. The constraint from x-ray observations of M31 from Horiuchi et al. [7] is denoted by the dashed (green) line, with a notable upturn at the signal region. The five stars produce the phase-space distributions shown in Fig. 2, and the three solid stars produce the linear WDM power spectrum transfer functions in Fig. 3. The contours change their orientation because the primary temperature of resonant production of the sterile neutrinos changes from prior to the quark-hadron transition to after it with increasing lepton number, for the case of the standard crossover quark-hadron transition at $T_{\rm QCD} = 170\,{\rm MeV}$ [14].

Production Calculations.—To calculate the resonant production of the sterile neutrino, I follow the detailed resonant production calculations first performed in Ref. [5] and specified for properties of the quark-hadron transition in Ref. [14].

The resonance in the production of the sterile neutrinos has the momentum position of

$$\epsilon_{\rm res} \approx \frac{\delta m^2}{(8\sqrt{2}\zeta(3)/\pi^2)G_{\rm F}T^4 L}$$

$$\approx 3.65\left(\frac{\delta m^2}{(7{\rm keV})^2}\right)\left(\frac{10^{-3}}{L}\right)\left(\frac{170{\rm MeV}}{T}\right)^4, \quad (1)$$

where $\epsilon_{\rm res} \equiv p/T|_{\rm res}$ is the position of the resonance, and $\delta m^2 \equiv m_2^2 - m_1^2$, where m_2 is more identified with the sterile neutrino. Here, $L \equiv (n_{\nu_\alpha} - n_{\bar{\nu}_\alpha})/n_\gamma$ is the lepton number of the Universe prior to resonant production, relative to the photon number n_γ. Since the lepton numbers of interest are of order 10^{-4}, we define $L_4 \equiv 10^4 L$. Here, the calculation is done for the flavor $\alpha = \mu$, but the general

features of the calculation are independent of flavor. There are subtleties with the effects of quantum-Zeno-effect damping in the full quantum kinetic equations (QKEs) in the case of resonance [19], but tests with the full QKEs in the resonance find that a quasiclassical quantum-Zeno treatment of production (such as that adopted here) is appropriate [20]. Further tests of the production in these models with the full QKEs is warranted, but this is beyond the scope of this brief Letter.

As discussed in Ref. [5], as the Universe expands and cools with time, for a given δm^2, the resonance will sweep through the ν_α energy distribution function from low to high neutrino spectral parameter ϵ. Before peak production, the sweep rate is $d\epsilon/dt \approx 4\epsilon H(1 - \dot{L}/4HL)$, where $\dot{L}$ is the time rate of change of the lepton number resulting from neutrino flavor conversion, and H is the expansion of the Universe.

The dominant effect on production is the value of the lepton number, which in turn sets the required $\sin^2 2\theta$ to get the cosmologically observed $\Omega_{\rm DM}h^2$. Because of this dependence, and since the production is largely independent of the sterile neutrino particle mass, we fix 7.14 keV, and explore how production changes with different values of $L_4 = 4.2, 4.6, 7, 8,$ and 10, shown as stars in Fig. 1.

As discussed in Ref. [5], since the expansion rate scales as $H \sim T^2$, the prospects for adiabaticity (efficiency) of the resonance are better at lower temperatures and later epochs in the early Universe—all other parameters being the same—up until the lepton number is depleted and conversion ceases. This produces the increasing peak in the distribution function for $L_4 = 4.2$ and 4.6 models. For larger lepton numbers, the resonance through the momentum distributions is at lower temperatures, partially before and partially after the quark-hadron transition, which is readily seen in the scaling of Eq. (1). The quasi-isotemperature evolution of the Universe during and after the quark hadron transition due to the heating of plasma with quark, massive hadron, and pion disappearance at this time produces the step-function feature in the distribution functions seen in the $L_4 = 7, 8, 10$ cases, as shown in Fig. 2.

Linear Cosmological Structure Inferred Properties and Constraints.—The resonant production mechanism has been known since its introduction to produce thermally "cooler" distributions than in the Dodelson-Widrow mechanism [4]. To accurately determine the nature of the matter perturbations arising in these models, I calculate the evolution of the sterile neutrino dark matter perturbations for the three representative cases $L_4 = 4.6, 7,$ and 8, as in Ref. [21], using the numerical Boltzmann cosmological perturbation evolution solver CAMB [22]. The resulting suppression of perturbations relative to CDM, $T_s(k)^2 = P_{\rm WDM}(k)/P_{\rm CDM}(k)$, is shown in Fig. 3. The exact shape of the transfer functions are different from the case of thermal WDM [2], but can be fit by thermal WDM transfer functions, shown as dashed lines in Fig. 3. The
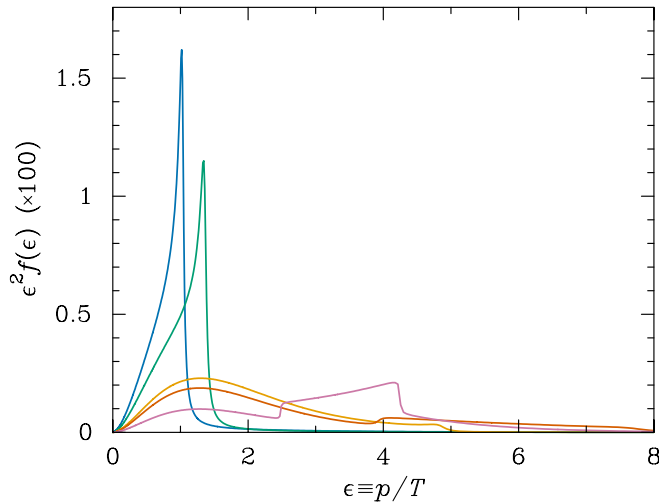
FIG. 2 (color online).   Shown here are the distribution functions of the 7.14 keV models shown as stars in Fig. 1. The models with $L_4 = 4.2$, 4.6, 7, 8, and 10 have, respectively, increasing average $\langle p/T \rangle$, and therefore larger-scale cutoffs in the linear matter power spectrum for the fixed particle mass. The 4.2 and 4.4 models have resonant production almost entirely prior to the quark-hadron transition, and therefore significantly "colder" properties than the remaining models, whose step-function-like features are due to the quasi-isotemperature evolution of the position of the resonance during the quark-hadron transition. All distributions are thermally cooler than the corresponding Dodelson-Widrow case, where $\langle p/T \rangle \approx 3.15$.

FIG. 3 (color online).   Shown here are the WDM sterile neutrino transfer functions $T_s(k) \equiv \sqrt{P_{\mathrm{WDM}}(k)/P_{\mathrm{CDM}}(k)}$ for the three solid stars in Fig. 1, as solid lines, with $L_4 = 8$, 7, and 4.6 having increasing k cutoff scales, respectively. Colors correspond to the distributions in Fig. 2. The dashed lines are the thermal WDM transfer functions that best fit these cases, which have a thermal WDM particle mass of $m_{\mathrm{thermal}} = 1.6$, 2.0, and 2.9 keV, respectively.

representative cases of $L_4 = 4.6$, 7, and 8 are best fit by thermal WDM particle masses of 1.6, 2.0, and 2.9 keV, respectively.

The most stringent claimed constraint on WDM is from observations and modeling of the Ly-α forest seen in spectra toward distant quasars. However, the Ly-α forest is a complicated tool for inferring the linear matter power spectrum, requiring disentangling the effects of pressure support and thermal broadening of the Ly-α forest features from the effects of dark matter perturbation suppression from WDM. In addition, modeling the dependence on the physics of the neutral gas requires assumptions of the thermal history of the intergalactic medium and its ionizing background. These are done as parametrized fitting functions. Many of the limitations of the Ly-α forest on constraints of the primordial power spectrum are discussed in Abazajian et al. [23]. The Ly-α forest modeling of the intergalactic medium and its numerical methods have considerably improved in recent years, and can provide stringent constraints that should be further studied regarding their robustness. Recent quoted limits are at thermal particle masses of $m_{\mathrm{thermal}} = 3.3$ keV (95% C.L.) [9].

Horiuchi et al. [7] studied in detail the phase-space constraints from Local Group dwarfs on Dodelson-Widrow sterile neutrino dark matter models. The warmest resonant dark matter model considered here, $L_4 = 10$, has a
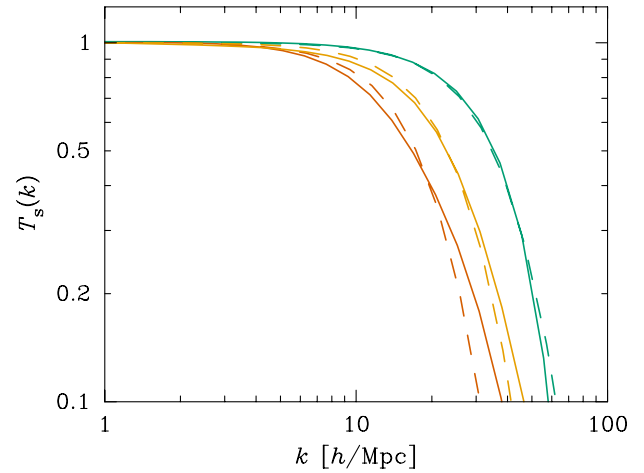
phase-space density $Q_{\mathrm{max}} \approx 398$, well above the minimum values inferred by Local Group dwarfs, e.g., Segue 1's requirement of $Q_{\mathrm{sim}} \approx 30$ [7]. Horiuchi et al. [7] and Polisensky and Ricotti [24] studied the constraints from the minimal subhalo number counts required to produce the observed dwarf galaxy populations of the Local Group. The constraint from subhalo counts in Horiuchi et al. [7] on Dodelson-Widrow sterile neutrinos corresponds to a thermal WDM particle mass of $m_{\mathrm{thermal}} = 1.7$ keV (95% C.L.). In addition, high-z galaxy counts exclude thermal WDM particle masses below $m_{\mathrm{thermal}} = 1.3$ keV at least at 2.2σ [25]. The high-z and Local Group subhalo constraints are in conflict with the warmest of the three resonant models for which we demonstrate the linear matter transformation function, $L_4 = 8$. The $L_4 = 4.6$ and 7 cases survive these structure formation constraints.

As shown in Fig. 1, the central $L_4 = 4.6$ case is in tension with the constraints from stacked x-ray observations of M31 [7]. The $L_4 = 7$ case is consistent with all Local Group structure formation and x-ray constraints, with a transfer function that matches that of thermal WDM of $m_{\mathrm{thermal}} = 2.02$ keV.

Perhaps most interestingly, the case of thermal WDM of $m_{\mathrm{thermal}} = 2$ keV is the cutoff scale inferred as a solution to the Milky Way satellite's total satellite abundance, the satellites' radial distribution, and their mass density profile, or the "too-big-to-fail problem," first discussed in Lovell et al. [18] and explored in detail in Anderhalden et al. [15], Polisensky and Ricotti [26], and Kennedy et al. [27]. Thermal WDM particle masses of $m_{\mathrm{thermal}} = 2$ keV are thought to not be significantly different from CDM in

subhalo kinematics (i.e., inner densities) [28]. These issues were also reviewed in detail in Ref. [29]. Overall, the range of thermal $m_{\text{thermal}} = 1.7$–2.0 keV is a "sweet spot" that may address the controversies in structure formation at small scales. Remarkably, as shown here, the cutoff scale of these WDM models is consistent with the preferred $L_4 \approx 7$ resonant sterile neutrino dark matter models of the unidentified x-ray line.

Conclusions.—Here I have presented the calculation of resonantly driven MSW-mechanism production of sterile neutrino dark matter that is in the parameter space of interest for the sterile neutrino dark matter decay interpretations of the recently reported unidentified x-ray line in x-ray clusters and M31, with the ansatz that sterile neutrinos are all of the dark matter. I have also presented the linear perturbation evolution and resulting transfer functions of the cool-to-warm resonant models that are consistent with the x-ray signal. Significantly, if the signal was slightly larger in $\sin^2 2\theta$ or m_s, then the effective thermal WDM mass would have been very cold and unconstrained, but commensurately of less interest. If $\sin^2 2\theta$ or m_s was slightly smaller, then the effective thermal WDM mass would have been very warm and constrained by several constraints that exist for WDM. However, the cutoff of the perturbation dark matter power spectrum in these models straddles exactly the region of interest necessary to alleviate structure formation controversies at small scales, corresponding to thermal WDM particle masses of 1.7 to 2.9 keV. The lepton-number model with $L_4 = 7$ is consistent with producing the 3.57 keV x-ray line, has a linear structure cutoff that matches that of thermal WDM particle masses of 2 keV, and is consistent with constraints from the Local Group, high-z galaxy counts as well as other x-ray constraints. Further tests of whether the Ly-α forest constraints are robust in this parameter space are certainly warranted.

The confirmation or exclusion of the x-ray line as originating from dark matter is certainly of great interest. This has been discussed in the literature, and tests of the dark matter's origin may be done via (i) x-ray observations of more Local Group galaxies [30], (ii) an energy resolution of the line to have dark-matter-velocity broadening instead of thermal broadening of a plasma line with the upcoming Astro-H mission [12], or (iii) an accurate determination of the flux profile of the line which could distinguish it from the plasma line's flux profile, as well as dark matter models that involve two-body processes and therefore a density-squared profile [31]. Lastly, to connect the x-ray line feature to the neutrino sector, it is arguable that it should be confirmed, e.g., by kink searches in nuclear β-decay spectra [32].

Thinking further ahead, as discussed in Ref. [14] and discussed above, if the 7 keV sterile neutrino is determined to be the dark matter, and the properties of the sterile neutrino required to produce the signal are sufficiently well determined, then one could hope to eventually test the nature of the quark-hadron transition which occurs during the resonant sterile neutrino dark matter production, since its properties affect the production.

It remains to be seen if the consistency between the unidentified x-ray line with small-scale structure formation considerations is either a mere coincidence or the emergence of a convergence of astrophysical methods of determining the nature of dark matter.

[1] G. R. Blumenthal, H. Pagels, and J. R. Primack, Nature (London) **299**, 37 (1982).

[2] P. Bode, J. P. Ostriker, and N. Turok, Astrophys. J. **556**, 93 (2001).

[3] S. Dodelson and L. M. Widrow, Phys. Rev. Lett. **72**, 17 (1994).

[4] X.-d. Shi and G. M. Fuller, Phys. Rev. Lett. **82**, 2832 (1999).

[5] K. Abazajian, G. M. Fuller, and M. Patel, Phys. Rev. D **64**, 023501 (2001).

[6] K. Abazajian, G. M. Fuller, and W. H. Tucker, Astrophys. J. **562**, 593 (2001).

[7] S. Horiuchi, P. J. Humphrey, J. Oñorbe, K. N. Abazajian, M. Kaplinghat, and S. Garrison-Kimmel, Phys. Rev. D **89**, 025017 (2014).

[8] U. Seljak, A. Makarov, P. McDonald, and H. Trac, Phys. Rev. Lett. **97**, 191303 (2006).

[9] M. Viel, G. D. Becker, J. S. Bolton, and M. G. Haehnelt, Phys. Rev. D **88**, 043502 (2013).

[10] I. Affleck and M. Dine, Nucl. Phys. **B249**, 361 (1985).

[11] M. Laine and M. Shaposhnikov, J. Cosmol. Astropart. Phys. 06 (2008) 031.

[12] E. Bulbul, M. Markevitch, A. Foster, R. K. Smith, M. Loewenstein, and S. W. Randall, arXiv:1402.2301.

[13] A. Boyarsky, O. Ruchayskiy, D. Iakubovskyi, and J. Franse, arXiv:1402.4119 [Phys. Rev. Lett. (to be published)].

[14] K. N. Abazajian and G. M. Fuller, Phys. Rev. D **66**, 023526 (2002).

[15] D. Anderhalden, A. Schneider, A. V. Maccio, J. Diemand, and G. Bertone, J. Cosmol. Astropart. Phys. 03 (2013) 014.

[16] M. Boylan-Kolchin, J. S. Bullock, and M. Kaplinghat, Mon. Not. R. Astron. Soc. **415**, L40 (2011).

[17] M. Boylan-Kolchin, J. S. Bullock, and M. Kaplinghat, Mon. Not. R. Astron. Soc. **422**, 1203 (2012).

[18] M. R. Lovell, V. Eke, C. S. Frenk, L. Gao, A. Jenkins, T. Theuns, J. Wang, S. White, A. Boyarsky, and O. Ruchayskiy, Mon. Not. R. Astron. Soc. **420**, 2318 (2012).

[19] D. Boyanovsky and C. Ho, J. High Energy Phys. 07 (2007) 030.

[20] C. T. Kishimoto and G. M. Fuller, Phys. Rev. D **78**, 023524 (2008).

[21] K. Abazajian, Phys. Rev. D **73**, 063506 (2006).

[22] A. Lewis, A. Challinor, and A. Lasenby, Astrophys. J. **538**, 473 (2000).

[23] K. Abazajian *et al.*, Astropart. Phys. **35**, 177 (2011).

[24] E. Polisensky and M. Ricotti, Phys. Rev. D **83**, 043506 (2011).

[25] C. Schultz, J. Oñorbe, K. N. Abazajian, and J. S. Bullock, arXiv:1401.3769.

[26] E. Polisensky and M. Ricotti, Mon. Not. R. Astron. Soc. **437**, 2922 (2013).

[27] R. Kennedy, C. Frenk, S. Cole, and A. Benson, arXiv:1310.7739.

[28] A. Schneider, D. Anderhalden, A. Maccio, and J. Diemand, arXiv:1309.5960 [Phys. Rev. Lett. (to be published)].

[29] D. H. Weinberg, J. S. Bullock, F. Governato, R. K. de Naray, and A. H. G. Peter, arXiv:1306.0913.

[30] A. Boyarsky, A. Neronov, O. Ruchayskiy, M. Shaposhnikov, and I. Tkachev, Phys. Rev. Lett. **97**, 261302 (2006).

[31] D. P. Finkbeiner and N. Weiner, arXiv:1402.6671 [Phys. Rev. D (to be published)].

[32] H. de Vega, O. Moreno, E. M. de Guerra, M. R. Medrano, and N. Sanchez, Nucl. Phys. **B866**, 177 (2013).